Proceedings of the 4th International Conference on Mechatronics and Smart Systems
DOI: 10.54254/2755-2721/2026.33561

Optical Biosensors Based on Bound States in the Continuum

Qianhong Guo

School of Physics & Electronic Science, Changsha University of Science and Enigneering, Changsha, China
20251103017@csust.edu.cn

Abstract. Bound states in the continuum (BICs) exhibit theoretically infinite quality factors and resonances that have ultra-narrow line widths, offering transformative potential the field of optical biosensing. This review surveys BIC-enabled biosensors and classify them by the type of materials used: metallic, all-dielectric, and metal-dielectric hybrid. This paper fist discusses BICs and how they can be categorized. Symmetry-protected and accidental BICs (such as Fabry-Pérot and Friedrich-Wintgen BICs) are discussed, and how the asymmetry of the structure can be used to explain the sensing performance of the structure using a coupled mode theory framework. Classically defined core performance metrics, i.e., quality factor, sensitivity, full width at half maximum, and figure of merit, are elaborated. Metallic BICs take advantages of plasmonic near field enhancements for low detection limits, but are limited by Ohmic losses. All-dielectric BICs achieve ultrahigh Q factors and topological robustness from Mie resonances, and hybrid systems combine the sensitivity of plasmonics with the high quality factor (Q factor) confinement of dielectrics. A range of state-of-the-art applications range from tumor phenotyping to exosome detection. Current capabilities BIC-enabled optical biosensors and analyze their potential are also assessed. Principal challenges the principal challenges ahead are highlighted, emphasizing on machine learning based designs to assist with BICs, microfluidic on-chip integration, and biosensing with gradients. These suggested technical advancements/ideas would provide the essential features to develop the intelligent biosensing systems of the future.

Keywords: Bound states in the continuum, Optical biosensor, Quasi-BIC, Quality factor

1. Introduction

Ultrasensitive sensors can identify biomolecules, chemical species, and associated substances with a level of accuracy never before seen. They have evolved, and this represents a significant breakthrough in chemical and biological detection [1]. Previous types - especially quartz crystal microbalance (QCM) instruments and electrochemical sensors - are limited by a lack of sensitivity, high prices, and time-consuming operational procedures. In comparison, optical sensors work based on the resonance-enhanced light-matter interactions. Some of the proven optical sensing platforms include surface plasmon resonance (SPR) sensors and dielectric guided-mode resonance (GMR) sensors [2]. Since the localization of the electromagnetic field is very strong, SPR is high-sensitivity; however, since dissipative loss is inevitably caused by metals, the Q-factor it can achieve

DOI: 10.54254/2755-2721/2026.33561

is decreased accordingly. Compared to SPR, GMR reduces energy dissipation thus giving rise to a smaller resonance linewidth. Nevertheless, although the Q-factor is greater, GMR is still limited by dielectric architectures, which, in turn, restrict the coupling to analytes.

Against this backdrop, BICs have drawn substantial interest because, in principle, they support an infinite Q-factor. A BIC may be understood as a resonant state characterized simultaneously by zero linewidth and zero radiation leakage [3]. With enhanced light-matter interaction and distinctive topological attributes, BICs allow sensor platforms to maintain strong robustness against perturbation. For that reason, BIC-based sensors have become a prominent subject of study in biosensing and related areas. In material terms, BIC sensors are commonly divided into three broad classes: metallic, all-dielectric, and hybrid. The present review offers a systematic examination of optical biosensors built on the physics of bound states in the continuum. At the outset, the physical origins of, and excitation pathways for, several BIC classes are outlined, covering not only symmetry-protected BICs but also accidental forms, including Fabry-Pérot and Friedrich-Wintgen configurations. Thereafter, a coupled-mode theoretical framework is introduced; structural asymmetry, treated here as a tuning parameter, is used to clarify how Q-factor evolution proceeds and how that evolution translates into biosensing-performance indices. From the standpoint of constituent materials, BIC-enabled biosensors are then organized into three principal groupings. First come metallic BIC sensors, whose architectures take advantage of plasmonic near-field enhancement while remaining constrained by Ohmic loss. Second are all-dielectric BIC sensors, in which Mie-type resonances supported by high-index media permit exceptionally high Q-factors together with topological protection. The third group consists of hybrid metal-dielectric BIC sensors, designed to unite, within a single platform, high sensitivity and elevated Q-factors. For each category, the discussion identifies the governing physical mechanisms and the relevant design heuristics. Representative structural implementations, along with state-of-the-art biosensing applications, are likewise catalogued.

Against this backdrop of the considerations of analysis presented above, a number of unsolved bottlenecks, and with them, possible lines of future study - take on a somewhat clearer form: machine-learning-assisted inverse design in the direction of more intelligent optimization; on-chip microfluidic integration in the direction of point-of-care testing; and the current move towards multimodal sensing platforms. Providing a comprehensive map of connections between the fundamental theory of the BIC and the real needs of biosensor engineering, this review serves as a theoretical background and as a technologically practical tool in the creation of the new generation and the high-performance optical biosensors.

2. Principle of BIC

BICs are spatially localized states of waves, which are confined even when they coexist with a continuum of other radiative modes. The radiation emitted in specific resonant states of periodic structures with a spatial symmetry is canceled by symmetry matching (as shown in Fig. 1) and therefore allows photon confinement. In a periodic system of this type, the spectrum does include a continuum which includes a multiplicity of spatially extended states (blue) - and bound states with discrete energy levels which do not emit outward flux (green). In these bound states, localization of space is due to the confining structure or, put somewhat more mechanically, due to the potential well (black dashed line). In comparison, states imbedded in the continuous spectrum are generally coupled to long waves and radiated, thus creating leaky resonant states (orange).

Of particular interest, bound states in the continuum (BICs, blue) constitute a distinct category: although positioned inside the continuum and coexisting with extended waves, they remain perfectly

DOI: 10.54254/2755-2721/2026.33561

confined and radiation-free. The diagram represents the classic picture. Such idealized BICs are also termed dark states [4]. In applied settings, however, the radiative counterpart namely, the quasi-BIC is of greater relevance. Through adjustment of structural parameters, including geometry, size, or material loss, the BIC can be made to couple weakly to the radiation continuum, so that a small fraction of its energy leaks outward; this weakly radiating state is designated a quasi-BIC [5]. As an ideal limit, BICs possess an infinite Q-factor. They cannot be excited by far-field plane waves, they do not couple to far-field radiation, and they therefore do not appear in the spectrum. Quasi-BICs, by comparison, do couple to the far field and exhibit partial leakage. Resonant damping is therefore present, and a nonzero resonant linewidth appears in the spectrum.

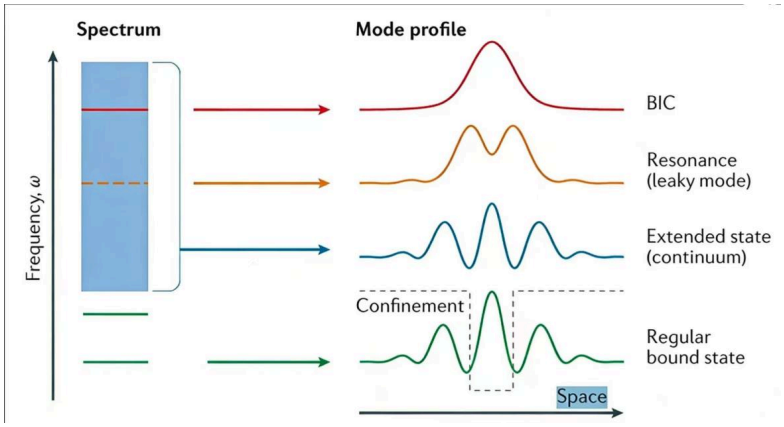

Figure 1. Schematic illustration of BICs

BICs can be mainly divided into two categories, as shown in Fig. 2. The first type is symmetry-protected BICs, which are caused by symmetry breaking. The second type is divided into resonant coupled-mode BICs and single-resonance BICs according to the interference of one or more waves. The resonant coupled-mode BICs can be further divided into Fabry-Pérot BIC and Friedrich-Wintgen BIC.

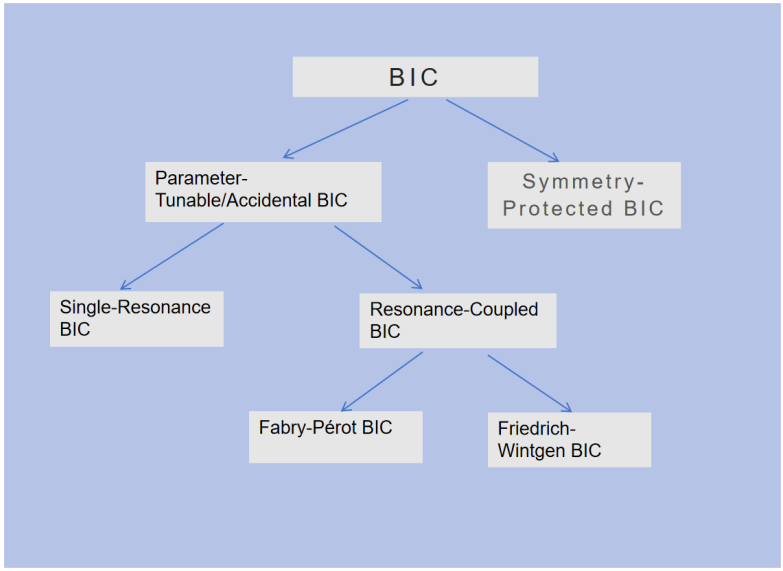

Figure 2. Classification of BICs

DOI: 10.54254/2755-2721/2026.33561

2.1. Symmetry-protected BICs sensors

When a system possesses reflection or rotational symmetry, modes belonging to different symmetry classes become fully decoupled. For example, a bound state in one symmetry class can be embedded within the continuum of another symmetry class, as long as the symmetry is preserved, the coupling between the two classes of modes is strictly forbidden. The "Γ" point is the central origin of the first Brillouin zone, corresponding to the position where the wavevector k = 0. Any mode at the Γ point that is symmetry-mismatched with respect to the radiation continuum can be a BIC. Away from the Γ point, these states begin to couple with radiation as they are no longer strictly protected by symmetry. Therefore, researchers can establish quasi-BICs by breaking spatial symmetry through adjusting the geometric parameters of the unit structure (e.g., positional offsets, dimensional differences). Examples include τ-shaped rectangles, and asymmetric crosses with offset center positions, among others [6,7]. The Q-factor of symmetry-protected quasi-BICs is closely related to the degree of symmetry breaking. Some studies use $Q=Q_0\alpha^{-2}$ to denote this correlation. Q_0 is a structure-dependent constant, and α represents the asymmetry parameter. Studies have found that Q decreases as α increases. A further increase in asymmetry beyond a critical threshold leads to a transition away from the quasi-BIC regime.

2.2. Accidental BIC sensors

When two or more resonant modes couple, destructive interference among their radiation channels can completely suppress radiation loss, giving rise to an accidental BIC. These are further classified into resonantly coupled BICs and single-resonance BICs.

2.2.1. Resonantly coupled BICs

Fabry-Pérot BICs arise from structures that form an effective Fabry-Pérot cavity (e.g., a bent waveguide with two reflecting interfaces). When the round-trip phase shift is an integer multiple of 2π, radiation from different channels cancels in the far field.

Friedrich-Wintgen BICs occur when two resonances coexist at the same spatial location and their radiation fields cancel through destructive interference, leaving one mode as a BIC and the other as a leaky resonance [8].

2.2.2. Single-resonance BICs

Even a single resonance can evolve into a BIC if it can be decomposed into multiple wave components (e.g., different multipole orders) whose far-field interference leads to complete destructive cancellation. Such BICs are often topologically protected and robust against structural perturbations, as demonstrated in photonic crystal slabs. Their existence and annihilation are governed by topological charges [9].

3. Sensing principle based on BICs

Quasi-BICs exhibit a strong response to refractive index variations. This property enables the efficient detection of dielectric environment changes caused by biomarker binding to the sensor surface, as well as refractive index fluctuations near the resonant structure. Such refractive index changes simultaneously induce a shift in the resonant wavelength and a variation in the Q - factor.

DOI: 10.54254/2755-2721/2026.33561

The small resonant wavelength displacement caused by a slight refractive index variation can be sensitively detected, leading to an ultralow detection limit. Furthermore, the strong localization effect of BIC enhances the interaction between the sensor and analytes, leading to ultrahigh sensing sensitivity. This confinement leads to a significant reduction in the mode volume V_{mode}, with a corresponding increase in the intensity of the localized field.

In a typical sensing configuration, an increase in the ambient refractive index results in a redshift in the resonance position. As S=Δλ/Δn, an increase Δn in the surrounding refractive index results in a proportional rise in neff and a shift Δλ in the resonance wavelength.

For symmetry-broken quasi-BICs, increasing the asymmetry parameter α (e.g., by introducing structural offsets) typically leads to a modest sensitivity improvement but at the cost of a drastic reduction in the Q-factor, as described by $Q \propto \alpha^{-2}$.

4. Definition of sensor performance indicators

1.Q factor: measures the ratio of stored energy to loss in the resonant state. $Q = \omega_0/(\gamma + \gamma')$. The higher the Q factor, the lower the energy loss and the narrower the spectral linewidth, resulting in stronger anti-interference capability and stability of the sensor.

2.Sensitivity (S): describes the sensor's responsiveness to variations in the refractive index. $S = \Delta\lambda/\Delta n$. where Δλ denotes the wavelength shift of the resonance peak, and Δn represents the change in the ambient refractive index.

3.Full width at half maximum (FWHM): refers to the spectral linewidth at half the peak intensity of the resonance, which directly determines the resolution of the sensing signal - the narrower the linewidth, the lower the detection limit.

4.Figure of merit (FOM): a core metric for comprehensively evaluating sensing performance, defined as FOM = $S / FWHM$. The higher the FOM value, the better the comprehensive performance of the sensor.

5. Classification of BIC sensors

5.1. Metallic BIC sensors

Metal-based SPR sensors are widely used due to their high refractive index sensitivity. However, Ohmic losses in metals severely limit their Q-factor, typically to the order of 10^2-10^3, which is far below that of all-dielectric counterparts. Introducing BICs into metallic systems can enhance both the Q-factor and FOM while preserving the intrinsic high sensitivity of metallic structures.

Metallic nanostructures support localized surface plasmon resonances (LSPR), which enhance the electromagnetic field and modify absorption, transmission, and reflection spectra - enabling biomolecule detection. The LSPR response of a metallic spherical nanoparticle (radius a ≪ λ) can be described by the resonance frequency:

$$\omega_\iota = \omega_p\left[\frac{\iota}{\varepsilon d(\iota+1)+\iota}\right]^{\frac{1}{2}} \quad (1)$$

where ω_p is the plasma frequency, εd is the dielectric constant of the surrounding environment, and ι is the angular momentum quantum number of the resonant mode. By introducing structural asymmetry, inter-element interference, or multipole cancellation, radiation channels can be completely suppressed, giving rise to plasmonic BICs or quasi-BICs.

DOI: 10.54254/2755-2721/2026.33561

When the ambient refractive index nd = εd changes, the LSPR wavelength shifts. The sensitivity can be approximated as:

$$S = \frac{d\lambda_{LSPR}}{dn_d} \approx \frac{\lambda_{LSPR}}{n_d} \bullet \frac{\varepsilon\infty+2n_d^2}{2n_d^2} \quad (2)$$

where LSPR is the high-frequency dielectric constant. This high sensitivity to the ambient refractive index is a key feature of LSPR, and it is retained in plasmonic BIC sensors.

In metallic architectures, BIC formation is achieved chiefly through the suppression of radiative leakage via symmetry breaking or inter-mode coupling, thereby supporting high-Q quasi-BIC resonant states. As dictated by the loss budget of the system, the Q factor is governed jointly by dissipative material absorption and radiation-induced loss.

Various metallic BIC-based biosensors have been reported, among them symmetry-broken terahertz metasurfaces and nanoscale metasurfaces. Of the symmetry-protected BIC implementations most commonly cited, two stand out:

Periodic gratings, owing to their readily traceable Q-factor dependence on asymmetry parameters, allow performance to be tuned in a comparatively predictable manner.

By contrast, nanorod and nanodisk arrays provide tighter near-field confinement and a smaller mode volume than gratings, thereby promoting more efficient analyte coupling. For the detection of relatively large biological targets - for example, viruses and exosomes in the 50-200 nm range - this wider-area field distribution is particularly advantageous.

Friedrich–Wintgen BICs in metallic architectures are, in most cases, implemented through dual-mode coupling configurations - metallic dimers, metal - dielectric hybrid platforms,and metallic nanoantennas. In 2025, Xu et al. employed metallic L-shaped resonators that supported a quasi-BIC state, with the associated Fano resonance positioned at 0.92 THz. Through geometric-parameter optimization, the Q-factor was rendered tunable. As for sensing performance, the device discriminated colorectal adenoma cells, which produced a 40 GHz resonance shift, from carcinoma cells, which induced a 60–80 GHz shift; linewidth broadening, additionally, tracked variations in cell permittivity. Taken together, these results establish a label-free route for rapid tumor phenotyping [10].

In 2023, Wang et al. designed a gold nanodisk dimer structure that supports a Friedrich - Wintgen quasi-BIC. This sensor achieves a Q - factor exceeding 800 in the near infrared region, a sensitivity of 510 nm/RIU, and a detection limit of 0.5 pg/mL for alpha - fetoprotein (AFP). For C-reactive protein (CRP) and serum amyloid A (SAA), a sensitivity slope of 674 GHz/RIU and a detection limit of 1 pM were demonstrated. The strong near-field enhancement ("hot spot") in the dimer gap (enhancement factor >10^5) combined with the narrow linewidth enables an aM (10^{-18} M) detection limit for certain analytes. This work shows that mode interference in metallic structures can yield Q-factors exceeding conventional LSPR while preserving high surface sensitivity [11].

5.2. All-dielectric BIC sensors

All-dielectric BIC sensors employ high-refractive-index dielectric materials (e.g., silicon, gallium arsenide, silicon nitride) to construct subwavelength resonant structures. Dielectric materials exhibit negligible Ohmic loss in the visible and near-infrared regions; thus, their intrinsic Q-factor is limited only by radiation loss. By suppressing radiation loss via the BIC mechanism, the Q-factor can theoretically reach 105 or even higher.

DOI: 10.54254/2755-2721/2026.33561

The physical mechanism underlying all-dielectric BICs is Mie resonance. Under illumination, high-refractive-index dielectric nanostructures support multiple multipole modes (electric dipole, magnetic dipole, electric quadrupole, etc.) arising from circular displacement currents. These modes have distinct radiation patterns and symmetries. By carefully designing the structure, destructive interference among their radiation fields can be achieved, leading to BIC formation.

The ultrahigh Q-factor enabled by low material loss significantly improves spectral resolution and lowers the detection limit. Unlike metallic BICs, which are sensitive to structural perturbations due to Ohmic losses, all-dielectric BICs - especially topological BICs in photonic crystal slabs - exhibit robustness against fabrication imperfections; the BIC persists, with only its momentum-space position shifting.

In 2025, Liu et al. designed a silicon elliptical cylinder array on a flexible polyimide substrate, achieving an accidental BIC by tuning the ellipse aspect ratio. This design achieved highly sensitive and repeatable detection of biomolecules in liquids (1pg/mL-1mg/mL) and ethanol solutions (concentration gradient of 20%-99.7%) [4].

In 2025, Ma et al. described an all-dielectric chiral metasurface built from circular apertures patterned in a monoclinic lattice. In the vicinity of the BIC regime, the far-field polarization undergoes rotation about a singular point, yielding a pronounced circular dichroism (CD) response; crucially, that response arises from the concurrent excitation of electric and magnetic dipoles, a coupled mechanism that metallic BIC platforms - being largely governed by electric-dipole excitations - do not realize. On this basis, the platform was used to detect bovine serum albumin (BSA) across a concentration window of 0.3-30 mg/mL, with a sensitivity of 0.023 (mg/mL). By simplifying fabrication while also lowering cost, the design moves commercial chiral sensing closer to practical deployment [12].

5.3. Hybrid metal-dielectric BICs

All-dielectric BICs are capable of reaching ultrahigh Q-factors; by comparison, the associated near - field enhancement remains relatively modest. In metallic BIC platforms, stronger near-field confinement and greater sensitivity to surface-bound analytes can indeed be obtained, although these gains are persistently constrained by intrinsic metallic loss. Positioned between these two architectures, hybrid BIC sensors seek to draw on the principal strengths of each, using metal-dielectric coupling configurations to realize a coupled - one might say deliberately co-optimized - combination of high Q - factor and high sensitivity.

Within the functional architecture of hybrid BIC sensors, the metal layer serves chiefly to excite surface plasmon resonance, thereby furnishing a highly sensitive response to analytes located at or near the surface. Once analyte molecules adsorb onto the metal interface, local variation in the metal dielectric constant alters the plasmon-resonance condition in a pronounced way, producing a resonance shift that can be directly measurable.

In comparison, the dielectric layer is mainly a high-Q resonant cavity. Symmetry breaking or, in certain designs, multipole - interference - suppressed radiative leakage is reduced, the resonance linewidth is decreased accordingly and spectral resolution is enhanced.

In 2025, Jia et al. developed a double-sided BIC metasurface biosensor for one-step differentiation of gastric cancer exosome subtypes. The metasurface is made of two layers of asymmetric split-ring resonators on a quartz substrate, both functionalized with two antibodies (anti-CD97 and anti-HMGB1). The exosomes that have been labeled with gold nanoparticles interact with the corresponding surfaces, resulting in different frequency shifts in two relative quasi-BIC resonances (QBIC I and QBIC II). This allows the detection of two exosomal membrane proteins

DOI: 10.54254/2755-2721/2026.33561

simultaneously. The platform shows a dynamic range of 1×10^4 to 1×10^8 particles/mL and a limit of detection (LOD) of 1×10^4 particles/mL, offering a novel approach for tumor subtype identification and personalized therapy [13].

Conventional BIC sensing has conventionally relied on monitoring resonance-wavelength changes, a measurement scheme that in practice requires high - resolution spectrometers and by definition limits sensor miniaturization. It is against this instrumentation bottleneck that Sun et al. (2024) developed a Q- switching-based sensing mechanism where the real component of the refractive index perturbs a loss in the oscillator damping and hence amplifies the peak. The strategy was implemented in a three-dimensional hybrid BIC metasurface produced by wafer-scale aluminum nanoimprinting, and achieves a peak-intensity sensitivity of 928%/RIU. Still contributing to this, the high Q factor provides a higher sensitivity without sacrificing compatibility with broadband light sources, a further combination that provides an actual route towards compact-system integration.

This miniaturized platform achieves a sensitivity of 928%/RIU and a detection limit of 129 aM in extracellular vesicles, orders of magnitude lower than the state-of-the-art biosensors. Combined, these findings show a lot of potential in home-based cancer care and in postoperative follow-up (especially in cases, where small formats of analysis are required) [14].

5.4. Summary and comparison of BIC sensor platforms

Table 1. Comparison of metallic, alldielectric, and hybrid BIC biosensor platforms

Feature / Platform	Metallic BIC Sensors	AllDielectric BIC Sensors	Hybrid MetalDielectric BIC Sensors
Material Basis	Plasmonic metals (Au, Ag, Al)	Highindex dielectrics (Si, GaAs, Si_3N_4)	Metaldielectric multilayers / composites
Primary Mechanism	LSPR	Mietype multipole resonances & interference	Coupling between plasmonic & dielectric modes
Typical QFactor	Moderate (10^2-10^3)	Ultrahigh (10^4-10^5)	High (10^3-10^4)
Sensitivity	High surface sensitivity (bulk: 100–600 nm/RIU)	Moderate to high bulk sensitivity (100–500 nm/RIU)	High sensitivity, often exceeding individual counterparts
NearField Enhancement	Very strong ("hot spots", $>10^4$)	Moderate (distributed mode volume)	Strong, enhanced in hybrid gaps / interfaces
FOM	Limited by moderate Q (10^2-10^3 RIU^{-1})	Very high due to ultranarrow linewidth ($>10^5$ RIU^{-1})	High, balancing sensitivity and linewidth ($>10^4$ RIU^{-1})
Loss Dominance	Ohmic loss (material absorption)	Radiation loss (suppressed by BIC design)	Combined Ohmic & radiation loss
Fabrication Complexity	Moderate (wellestablished EBL, nanoimprinting)	High (requires precise highindex patterning)	High (multistep alignment & material integration)
Topological Robustness	Sensitive to structural perturbations	Strong robustness, especially for topological BICs	Moderate, dependent on hybrid mode stability
Primary Application	Ultralow concentration detection (aM-fM); small molecules	Highresolution multiparameter sensing; chiral discrimination	Pointofcare diagnostics; exosome phenotyping; clinical assays

To provide a clearer basis for selecting an appropriate platform across distinct biosensing scenarios, the three principal classes of BIC sensors - metallic, all-dielectric, and hybrid metal-

DOI: 10.54254/2755-2721/2026.33561

dielectric configurations - are compared systematically in terms of their governing physical mechanisms, performance - defining attributes, fabrication requirements, and the application settings in which they are most commonly deployed.

At the level of operating principle, metallic BIC sensors are controlled by plasmonic resonances, which generate intensely confined local near-fields and therefore deliver exceptionally high surface sensitivity together with ultra-low detection limits. That advantage, familiar in plasmonic sensing, is paired with an equally familiar constraint: intrinsic Ohmic dissipation within the metal limits the attainable quality factor to the 10-10 range, thereby reducing suitability for sensing tasks that depend on exceptionally narrow spectral linewidths. By comparison, all-dielectric BIC sensors rely on Mie-type resonances sustained by low-loss, high-index materials; through that route, ultra-high Q-factors (10^{10}) and excellent spectral resolution can be achieved. Added to this is their topological robustness, a property that affords a measure of tolerance to fabrication-induced perturbations (though not an unlimited one, particularly when geometric control becomes decisive). Even so, the limitations remain easy to identify. Near-field enhancement is typically weaker, and the required nano-structuring often has to be carried out with considerable precision. Occupying an intermediate position rather than simply concatenating the two constituent design logics, hybrid metal-dielectric BIC sensors are intended to unite the high surface sensitivity associated with plasmonic elements with the high-Q resonant confinement provided by dielectric structures. In applied terms, this produces a more balanced performance profile-one that is especially appealing in complex, multi-parameter sensing settings. The trade-off, however, is not negligible: hybrid architectures usually involve greater fabrication complexity and, with the inclusion of metal components, reintroduce optical loss. Table 1 condenses the key attributes of these three BIC sensor platforms so that direct comparison becomes more straightforward.

When selecting a BIC sensor platform, the decisive criteria should be the demands imposed by the target analyte and the intended detection environment. For trace-level molecular detection, metallic BICs remain the strongest option because they deliver the lowest attainable detection limits. By contrast, all-dielectric BICs are distinguished by exceptional spectral resolution and operational stability, properties that make them especially well suited to precise quantification. Hybrid BICs, situated between these two design strategies, offer a more flexible balance - namely, integrated, high-performance biosensing capability under the challenging conditions posed by complex biological media.

6. Conclusion

This paper presents a systematic review of optical biosensors grounded in BIC. By material platform, these devices fall into three categories: metallic BIC, all-dielectric BIC, and hybrid BIC. For each class, the underlying physical mechanisms, structural realizations, performance profiles, and biosensing uses are examined in detail. In biosensing practice, these three BIC sensor types function in a complementary manner: metallic BIC is well suited to surface-sensitive, ultra-low-concentration detection; all-dielectric BIC better serves high-precision, multi-parameter, and long-term stable detection; hybrid BIC, by contrast, attempts to merge the advantages of both and therefore shows substantial promise for high-performance integrated sensing. Notwithstanding the considerable progress already achieved by BIC sensors in biosensing, practical clinical deployment and large-scale industrial translation still face a number of unresolved obstacles. Subsequent research may therefore be directed toward the following avenues: intelligent structures and inverse design, integration with microfluidics, multimodal sensing, and large-scale clinical validation.

DOI: 10.54254/2755-2721/2026.33561

The BIC metasurface sensors are moving towards intelligent and integrated systems. Machine learning can be used to do rapid inverse design. This is a de-bottleneck of the traditional parameter scanning. It accelerates sensor development. Combination with microfluidics and chips forms lab-on-a-chip devices. Such devices enable high throughput and automatic detection of trace samples. They bring BIC sensors nearer to point-of-care testing. Multimodal sensing involves the integration of BIC with other methods. Such methods are Raman spectroscopy and fluorescence imaging. They show complementary molecular data on a single platform. This enhances the level of accuracy in diagnosis. The majority of BIC sensors however are still in the form of laboratory prototypes. They require massive confirmation through actual clinical samples. The sensitivity and specificity of complex matrices are evaluated by such validation.

Finally, as micro/nanofabrication technologies, the incorporation of artificial intelligence in design, and a better comprehension of the physical processes of BICs are developed, high-performance optical sensors that utilize BICs are likely to be even more significant in biomedical research, clinical diagnostics, environmental measurements, and food safety. They are set to form the backbone of the next-generation ultrasensitive biosensing.

References

[1] Vafadar, A., Maleki, M., Ehtiati, S., Moghadam, H. Z., & Avardashtak, A. (2026). Optical biosensors for detection of exosomes. Clinica Chimica Acta, 579, 120704.https: //doi.org/10.1016/j.cca.2025.120704

[2] Thapa, D. K., & Biswas, S. (2025). Leveraging bound states in the continuum for advanced ultra-sensitive sensing technologies. Materials Horizons, 12, 5096-5122.https: //doi.org/10.1039/D5MH00413F

[3] Hsu, C. W., Zhen, B., Stone, A. D., Joannopoulos, J. D., & Soljačić, M. (2016). Bound states in the continuum. Nature Reviews Materials, 1, 16048. https: //doi.org/10.1038/natrevmats.2016.48

[4] Liu, Q., et al. (2025). Q-BIC THz metasurface biosensor based on flexible polyimide for solution detection. IEEE Sensors Journal, 25(7), 11008-11015. https: //doi.org/10.1109/JSEN.2025.3539525

[5] Lin, D., Ghaffari, A., & Gu, Q. (2025). Chiral metasurfaces with multidimensional tunability for optical chiral states. Advanced Optical Materials, 13(36), e01859. https: //doi.org/10.1002/adom.202501859

[6] Ma, T., Tian, J., & Li, J. (2023). Chiroptical resonances with high Q factors driven by quasi bound states in the continuum in all-dielectric metasurface at terahertz frequencies. Optics Communications, 532, 129216. https: //doi.org/10.1016/j.optcom.2022.129216

[7] Zhang, S., Fan, Y., Ma, Y., Zong, M., Sun, H., Yang, Z., & Xu, Z. (2026). Bound states in the continuum: From fundamental physics to emerging photonic paradigms. iScience, 29(2), 114803. https: //doi.org/10.1016/j.isci.2026.114803

[8] Zhao, X., Chen, C., Kaj, K., Hammock, I., Huang, Y., Averitt, R., & Zhang, X. (2020). Terahertz investigation of bound states in the continuum of metallic metasurfaces. Optica, 7(11), 1548-1554. https: //doi.org/10.1364/OPTICA.402169

[9] Chen, S., Zeng, Y., Li, Z., Mao, Y., Dai, X., & Xiang, Y. (2023). Passive nonreciprocal transmission and optical bistability based on polarization-independent bound states in the continuum. Nanophotonics, 12(18), 3613-3621. https: //doi.org/10.1515/nanoph-2023-0319

[10] Xu, H., Wang, H., Yang, X., Grønlien, I., Torvund, A. G. S., Xomalis, A., & Zhao, Z. (2025). Identifying phenotypes of colorectal malignant tumors using the quasi-bound state in the continuum of a terahertz metasurface biosensor. Biomedical Optics Express, 16(4), 1471-1482. https: //doi.org/10.1364/BOE.557218

[11] Wang, R., Xu, L., Huang, L., et al. (2023). Ultrasensitive terahertz biodetection enabled by quasi-BIC-based metasensors. Small, 19, 2301165. https: //doi.org/10.1002/smll.202301165

[12] Ma, T., Zou, Y., Chen, Z., Afzal, I., Kong, D., Wang, D., Ma, L., & Li, J. (2025). Resonant chiroptical effects in an all-dielectric metasurface with monoclinic lattices for terahertz sensing applications. Nanoscale, 17, 21837-21843. https: //doi.org/10.1039/D5NR02689J

[13] Jia, Q., Ma, Z., Wang, Y., Zhang, M., Zou, G., Lan, B., Li, S., Lao, Z., Shen, W., Lou, J., Jiao, Y., & Du, X. (2025). Integrated single-step terahertz metasensing for simultaneous detection based on exosomal membrane proteins enables pathological typing of gastric cancer. Research, 8, 0625. https: //doi.org/10.34133/research.0625

[14] Sun, J., Li, F., Wang, X., He, J., Ni, D., Wang, L., Lin, S., Min, Q., Zhu, J., & Wen, L. (2024). Loss-driven miniaturized bound state in continuum biosensing. arXiv preprint, arXiv: 2411.18110. https:

DOI: 10.54254/2755-2721/2026.33561

//arxiv.org/abs/2411.18110